European Journal of Pharmaceutical Sciences 202 (2024) 106891

Contents lists available at ScienceDirect

European Journal of Pharmaceutical Sciences

journal homepage: www.elsevier.com/locate/ejps

Spray drying of a zinc complexing agent for inhalation therapy of pulmonary fibrosis

Justin Stella [a], Maryam Ayman Mohamed Ezzat Abdelaal [a], Mohamed Ashraf Mostafa Kamal [a,b], Kristela Shehu [a,c], Alaa Alhayek [b,1], Jörg Haupenthal [b], Anna K. Hirsch [b,d], Marc Schneider [a,*]

[a] Department of Pharmacy, Biopharmaceutics and Pharmaceutical Technology, Saarland University, Campus C4 1, Saarbrücken 66123, Germany
[b] Helmholtz Institute for Pharmaceutical Research Saarland (HIPS) — Helmholtz Centre for Infection Research (HZI), Campus E8 1, Saarbrücken 66123, Germany
[c] INM – Leibniz Institute for New Materials, Saarbrücken 66123, Germany
[d] Department of Pharmacy, Medicinal Chemistry, Saarland University, Saarbrücken 66123, Germany

ARTICLE INFO

Keywords:
Pulmonary fibrosis
Phytic acid
Zinc chelator
Metalloproteinase enzymes
LasB
Spray drying
Aerodynamic properties

ABSTRACT

Pulmonary fibrosis, a disabling lung disease, results from the fibrotic transformation of lung tissue. This fibrotic transformation leads to a deterioration of lung capacity, resulting in significant respiratory distress and a reduction in overall quality of life. Currently, the frontline treatment of pulmonary fibrosis remains limited, focusing primarily on symptom relief and slowing disease progression. Bacterial infections with *Pseudomonas aeruginosa* are contributing to a severe progression of idiopathic pulmonary fibrosis.

Phytic acid, a natural chelator of zinc, which is essential for the activation of metalloproteinase enzymes involved in pulmonary fibrosis, shows potential inhibition of LasB, a virulence factor in *P. aeruginosa*, and mammalian metalloproteases (MMPs). In addition, phytic acid has anti-inflammatory properties believed to result from its ability to capture free radicals, inhibit certain inflammatory enzymes and proteins, and reduce the production of inflammatory cytokines, key signaling molecules that promote inflammation. To achieve higher local concentrations in the deep lung, phytic acid was spray dried into an inhalable powder. Challenges due to its hygroscopic and low melting (25 °C) nature were mitigated by converting it to sodium phytate to improve crystallinity and powder characteristics. The addition of leucine improved aerodynamic properties and reduced agglomeration, while mannitol served as carrier matrix. Size variation was achieved by modifying process parameters and were evaluated by tools such as the Next Generation Impactor (NGI), light diffraction methods, and scanning electron microscopy (SEM). An inhibition assay for human MMP-1 (collagenase-1) and MMP-2 (gelatinase A) allowed estimation of the biological effect on tissue remodeling enzymes. The activity was also assessed with respect to inhibition of bacterial LasB. The formulated phytic acid demonstrated an IC50 of 109.7 μg/mL for LasB with viabilities > 80 % up to 188 μg/mL on A549 cells. Therefore, inhalation therapy with phytic acid-based powder shows promise as a treatment for early-stage Pseudomonas-induced pulmonary fibrosis.

1. Introduction

Pulmonary fibrosis, a worldwide chronic disease, is a chronic and irreversible lung disorder with unknown etiology (Procaccini et al., 2019) characterized by the formation of scar tissue within normally functioning alveoli. Prominent symptoms include dry cough, dyspnea, shortness of breath, weight loss, fatigue, and impaired gas exchange (Glass et al., 2022). *Pseudomonas aeruginosa* (*P. aeruginosa*) has been identified as a causative factor (Moghoofei et al., 2022; Yamazaki et al., 2016). Advanced age, typically around 65 years, correlates with average onset, and patients survive an average of about five years after diagnosis (Glass et al., 2022). Notably, men are more susceptible to the disease, accounting for approximately 70 % of the patient population, often with a history of smoking, making smoking an additional risk factor for pulmonary fibrosis (Glass et al., 2022). Each year in the United States alone, 30,000 to 40,000 people are diagnosed with pulmonary fibrosis (Speca et al., 2020).

The primary intervention for pulmonary fibrosis is lung

* Corresponding author.
E-mail address: Marc.Schneider@uni-saarland.de (M. Schneider).
[1] Present address: Biozentrum, University of Basel, Basel, Switzerland

https://doi.org/10.1016/j.ejps.2024.106891
Received 17 April 2024; Received in revised form 24 August 2024; Accepted 1 September 2024
Available online 2 September 2024

transplantation. However, several alternative therapies are available to reduce symptoms and slow the progression of the disease, including lifestyle changes in patients, such as smoking cessation, dietary changes, and regular exercise (Gabardi et al., 2011). Exposure of lung cells to toxins or microbes triggers the release of cytokines by activated immune cells to combat factors such as *P. aeruginosa*, thereby enhancing the fibrotic process and escalating inflammation. This is followed by the activation and production of metalloproteinase enzymes and the release of hydroxy radicals (Huang et al., 2020). The progression of pulmonary fibrosis proceeds in three phases: initial injury, subsequent inflammation, and eventual repair. Upon exposure to a toxin or microbe such as SARS-CoV-2, the tissue attempts to self-heal and return to its original state. Host-related factors, specifically matrix metalloproteinases (MMPs), play an essential role (Cabral-Pacheco et al., 2020).

Matrix metalloproteinases (MMPs) are key enzymes involved in pulmonary fibrosis indicated by upregulation of many of the MMPs clearly hinting to a disbalance which is however complex in its nature (Pardo et al., 2016). Bacterial proteinases, such as LasB, share similarities with mammalian MMPs in their functional dependence on Ca^{2+} and Zn^{2+} and their broad target spectrum of extracellular components. Elastase B (LasB), a metalloprotease virulence factor produced by the Gram-negative bacterium *P. aeruginosa*, facilitates bacterial invasion of human tissues and extensive dissemination within the host. LasB cleaves extracellular matrix proteins, including elastin and collagen, allowing tissue invasion, and spread of infection. Furthermore, LasB is involved in evading the immune system, for example by degrading SP-A responsible for improved uptake (Everett and Davies, 2021; Ruge et al., 2011). Thus, LasB plays an important role in the development of chronic infections, particularly notable in diseases such as pulmonary fibrosis (Cabral-Pacheco et al., 2020; Everett and Davies, 2021; Saint-Criq et al., 2018).

The influence of the enzyme matrix metalloproteinase on the pathogenesis of pulmonary fibrosis has been confirmed (Inoue et al., 2023; Moghoofei et al., 2022). As a Zn^{2+}-dependent enzyme, it is triggered by Zn^{2+}, which initiates further activation by Ca^{2+} *via* its calcium-binding domain (Bormann et al., 2022). Zinc ions also play a key role in activating MMP-1 in human tissues and stabilizing its transition state during the reaction. For example, MMP-1 (collagenase-1) targets type 1 collagen, the most abundant protein in the extracellular matrix of animals and humans (Cabral-Pacheco et al., 2020). Similarly, MMP-3 (stromelysin-1) exhibits broad capabilities, cleaving various extracellular matrix components such as collagens and proteoglycans (Laronha and Caldeira, 2020). Unspecific blocking of MMPs did not lead to the expected outcomes (Pardo et al., 2016), which points towards the complex processes inducing effects on the extracellular matrix (ECM) but also on the modulation of cell behavior (Pardo et al., 2016). Nevertheless, the interference of the natural Zn^{2+}complexing agent phytic acid (Gupta et al., 2015) was envisaged as a potential onset evaluating the specific interaction with bacterial MMP (LasB). In general, phytic acid is found in whole grains (wheat, oats, and rice), legumes (kidney beans, soybeans, lentils), nuts, seeds, and potatoes (Oatway et al., 2001). It is the most common form of phosphorus storage connected to its chemical structure: myoinositol-1,2,3,4,5,6-hexakis dihydrogen phosphate (Gupta et al., 2015). Phytic acid is also known as inositol hexaphosphate (IP6) and can be dephosphorylated to IP3 (Silva and Bracarense, 2016), a signaling molecule in cells that has an important second messenger function. It acts on intracellular receptors to release Ca^{2+}, leading to various cellular responses (Chatree et al., 2020). This suggests a certain biocompatibility of IP6 in combination with the low membrane penetration ability due to its hydrophilicity and charge. Furthermore, phytic acid has immune-enhancing properties and protects against insulin resistance (Dilworth et al., 2023). Its antioxidant capacity prevents DNA breakage and the generation of iron-related hydroxy radicals, which cause cellular damage, as mentioned above (Aguree et al., 2020). In addition, phytic acid has anti-inflammatory properties by inhibiting cytokines involved in aggressive responses, such as NF-kappa B and TNF-alpha (Lv et al., 2015). These collective effects protect lung cells from fibrosis induced by prolonged inflammation, a benefit that might be achieved by inhaling phytic acid.

This study aims to test and provide an effective formulation to investigate a new onset for treating pulmonary fibrosis. For this purpose, phytic acid was formulated as an inhalable dry-powder formulation. Dry-powder inhalation therapy has many advantages, such as the controllability of particle deposition *via* the particle size; the application of a higher dose with simultaneous reduction of systemic side effects through local application, as well as the easy handling of the DPI device (Chrystyn and Lavorini, 2020). This formulation is designed to deliver phytic acid directly to the site of action to complex zinc ions and break the inflammatory cycle in pulmonary fibrosis.

Obstacles related to the hygroscopic nature and the low melting point of phytic acid were overcome and allowed dry powder formulation. The formulation was optimized and characterized for the powder properties such as particle sizes, morphology, and aerodynamic properties. To investigate the zinc chelation potential, a respective colorimetric assay was used. In addition, the biological activity of the formulation was verified using the LasB inhibition assay and testing for the activity of human proteases involved in pulmonary fibrosis (MMP-1 and MMP-2 inhibition assays). Finally, incubation of lung cells (A549) for estimating the biocompatibility of the formulation was performed.

2. Materials and methods

2.1. Materials

Phytic acid (dissolved in water, 1.1 mol/L) was purchased from Tokyo Chemical Industry (TCI) (Tokyo, Japan). α-Lactose monohydrate, D-mannitol, L-leucine, maltodextrin dextrose and trehalose were obtained from Sigma Aldrich (Steinheim, Germany). Sodium hydroxide and D(+)-trehalose dihydrate by Carl Roth (Karlsruhe, Germany). The zinc quantification kit ab176725 (Fluorometric) was purchased from Abcam (Berlin, Germany). Isopropanol, Acetone, and Brij®98 were obtained from Thermo Fisher Scientific Chemicals (Schwerte, Germany). 2-Aminobenzoyl-Ala-Gly-Leu-Ala-4-Nitrobenzylamide was from Peptides International (Louisville, KY, United States) and elastase was from Elastin Products Company (Owensville, MO, USA). The SensoLyte® 520 Generic MMP Activity Kit Fluorimetric was supplied by AnaSpec (Fremont, CA, USA).

2.2. Preparation of microparticles by spray drying

Various compositions of D-mannitol, L-leucine and phytic acid were tested. All components were first weighed together in a beaker. Pure MilliQ water and mixtures of 50 % v/v acetone in water or 50 % v/v isopropanol in water were used as spray medium. Liquid medium was added to obtain a solid content of the spray solution of 2 % (w/w). The mixture was stirred on a heating plate at 50 °C and 800 rpm for 15 min until all components were completely dissolved. To prevent the loss of solvent through evaporation, the organic solvent-containing spray media were dissolved in a sealed Schott bottle under identical conditions.

Once dissolved on the heating plate, the sample was allowed to cool down to room temperature (20 °C). The pH of the samples was then adjusted to 7.4 using 0.5 molar sodium hydroxide solution for spray drying. If the samples were used for the determination of aerodynamic properties using NGI, additionally 200 µL/100 mL of a 0.5 mg/mL Rhodamine B solution was added before spray drying for fluorometric quantification.

Spray drying was carried out using a B-190 spray dryer from Büchi (Flawil, Switzerland), operated at an inlet temperature at room temperature for the organic solvents and an inlet temperature of 66 °C for the aqueous solutions resulting in an outlet temperature of around 51 °C. The feed pump rate was 3.0 mL/min, the atomizing air flow rate was

~750 L/h and the aspirator operated at full capacity (~35 m^3/h). The powders were stored in a desiccator until further use.

To optimize the formulation and determine the process parameters, various batches with different compositions were spray dried. For selecting an appropriate spray medium, a solution of 5 w% phytic acid and 95 w% mannitol was prepared. For the identification of the most suitable excipient carrier, a solution of 5 % phytic acid was prepared by mixing with 95 % of the corresponding excipient. Mannitol, maltodextrin, lactose, and trehalose were employed for this objective (Table 1).

The optimization of the inlet temperature was conducted using a mixture of 15 % phytic acid and 85 % mannitol. The impact of varying the quantity of L-leucine on the quality and stability of the dry powder formulation was evaluated at a constant PA content of 15 %. L-leucine contents of 5, 10, 20 and 35 % were employed, with the remaining portion supplemented with mannitol. The optimal phytic acid content was tested at levels of 10, 20, 30 and 40 %. The L-leucine content was maintained at 20 % while the composition was filled with mannitol.

2.3. Particle size and size distribution analysis via laser light scattering

Two approaches were used to analyze the spray dried powder by laser diffraction. One was based on dispersing the powder in a relevant non-solvent and the other approach by dispersing the particles in an air stream.

First, 20 mg of the spray dried microparticle formulations were weighed into an Eppendorf vial and suspended in 4 mL of 1-octanol for 30 s using a vortex shaker. A Malvern Mastersizer 2000 was used to determine the particle size by laser light diffraction. The stirrer was set to 1000 rpm. The refractive index was selected according to the main component of the microparticle, usually the filling material. Literature values were used for this purpose. The refractive index for mannitol was 1.33 (Haynes et al., 2016), for maltodextrin 1.673, for trehalose 1.652 (CSID:158279 (accessed 16:38, Feb 19, 2024)), and for lactose 1.532 (Bushill et al., 1965). A refractive index of 1.451 was selected for the dispersion medium 1-octanol (Haynes et al., 2016). Second, the spray dried powder was analyzed by laser light diffraction using the Horiba Partica LA-950; in contrast to the Malvern Mastersizer 2000, the sample is dispersed via an air flow. Approximately 1000 mg of the microparticle formulation is added to the sample chamber and drawn in via an air flow of 150 liters per minute. Fraunhofer diffraction was used to calculate the particle size distribution.

2.4. Morphology analysis

The formulation was applied dry to a conductive carbon disc. The excess powder was carefully removed with compressed air so that only one microparticle layer remained on the disc surface. To improve image quality, a 10 nm gold layer was deposited using a Quorum Q150R ES sputter coater (Quorum Technologies Ltd, East Grinstead, UK). The morphology and size of the formulation was analyzed using a Zeiss EVO HD 15 scanning electron microscope (SEM) (Zeiss, Oberkochen, Germany). An acceleration voltage of 5.0 kV was used.

Table 1
Overview of the excipients utilized and the corresponding sample compositions.

Sample name	PA (w %)	Mannitol (w%)	Lactose (w%)	Trehalose (w%)	Maltodextrin (w%)
5 %PA95 %mann	5	95	–	–	–
10 %PA85 %mann	10	90	–	–	–
15 %PA85 %mann	15	85	–	–	–
5 %PA95 %lac	5	–	95	–	–
5 %PA95 %treh	5	–	–	95	–
5 %PA95 %malt (4–7)	5	–	–	–	95
5 %PA95 %malt (16.5–19.5)	5	–	–	–	95

2.5. Evaluation of aerodynamic properties

The Next Generation Impactor (NGI) is a seven-stage impactor that can be used to test the aerodynamic properties of dry-powder formulations. A Brij solution was first applied to the inner surface of the NGI cups. This surface treatment prevents rebound effects that could affect the deposition results similar to the liquid coated biological interfaces. The solution was left to dry on the cups to allow the particles to adhere to the cup surface. The Brij solution was prepared by adding 7.5 g of Brij®35 to 50 mL of ethanol (96 % v/v) and stirring at 800 rpm for 30 min at 30 °C. Then 40 mL of this solution was added to 60 mL of glycerol. Thus, the Brij solution consists of 40 % v/v ethanol and 60 % v/v glycerol. A size 3 gelatin capsule was filled with 20 mg of the powder formulation. This gelatin capsule was then placed in a HandiHaler® (Boehringer Ingelheim, Ingelheim, Germany) and pierced to allow release of the dry powder formulation. The airflow was adjusted to 60 L/min, which corresponds to the peak respiratory flow rate in humans (Buttini et al., 2016). The airflow was forced by the vacuum pump (Erweka, Heusenstamm, Germany) for 4 s. Finally, the NGI was disassembled and the deposited sample from each cup was dissolved in 10 mL Milli-Q water. The same treatment was carried out for the throat part and the capsule. In contrast, the powder fraction deposited in the induction port was dissolved in 30 mL of Milli-Q water. From the tested formulations (containing Rhodamine B), dilutions of known concentrations were prepared and used to construct a calibration curve. For this purpose, the dilutions were measured with the Tecan Reader Infinite 200 (Tecan, Männedorf, Switzerland) using an excitation value λ_{ex} of 565 nm and an emission value λ_{em} of 625 nm, corresponding to the dye used (Rhodamine B). All experiments were performed in triplicate under constant conditions.

2.6. Measurement of the moisture content

The moisture content of the spray-dried formulations containing mannitol at different concentrations (40 - 70 %) was performed via thermogravimetric analysis (Sartorius MA37–1, Sartorius AG, Göttingen, Germany). Formulations were weighed and placed uniformly in the sample pan. The moisture content (%) was determined as the weight loss registered during the drying process (130 °C).

2.7. Stability over time

The physical stability of the formulations (freshly prepared and stored for more than a year in the desiccator) was measured via X-Ray Powder Diffraction (XRD) by using a Bruker D8 Advance diffractometer (Bruker, Ettlingen, Germany).

2.8. Evaluation of zinc ion quantification and phytic acid binding capacity

A fluorometric zinc quantification kit (ab176725) from Abcam (Berlin, Germany) was used to determine Zn^{2+} concentrations and to assess the zinc chelating capacity of phytic acid. The zinc assay detector was prepared by adding the zinc probe (25 µL) to the assay buffer (5 mL). The zinc detector then complexes with Zn^{2+} in the solution and this interaction is allowed to occur for 5–10 min at room temperature. Quantification of the resulting amounts was performed using a Tecan Infinite 200 reader (Tecan, Männedorf, Switzerland), measuring fluorescence at an excitation wavelength $\lambda_{ex} = 485$ nm and an emission wavelength $\lambda_{em} = 525$ nm.

2.9. Molecular conformation simulation of zinc ions and phytic acid

First, two phytic acid molecules were drawn together with eight Zn^{2+}

ions and run on Molecular Operating Environment (MOE) version 2020. The software then performed a stochastic conformation search using all default settings except for the rejection limit, which was set to 1000. The best conformer was reused and then plotted again on the MOE. Another conformation search was performed using "lowMD" setting. The default setting was used except for the rejection limit, which was set to 1000.

2.10. LasB inhibition assay

The LasB assay involves the binding of an enzyme to a substrate, resulting in the formation of an enzyme-substrate complex and subsequent cleavage of the substrate. The substrate, when cleaved in the presence of an inhibitor, produces fluorescence. Conversely, in the absence of inhibition, the substrate remains intact and does not fluoresce. This fluorescence dynamic allows monitoring of enzyme activity within the LasB assay (Kolling et al., 2023).

LasB was expressed and purified according to previously documented procedures (Kany et al., 2018). Fluorescence intensity measurements were performed in black 384-well microtiter plates (Greiner BioOne, Kremsmünster, Austria) for 60 min at 37 °C, using an excitation wavelength $\lambda_{ex} = 340 \pm 15$ nm and an emission wavelength $\lambda_{em} = 415 \pm 20$ nm. The CLARIOstar microplate reader (BMG Labtech, Ortenberg, Germany) was used for data acquisition.

The assay buffer composition (50 mM Tris, pH 7.2, 2.5 mM $CaCl_2$, 0.075 % Pluronic F-127, 5 % DMSO) had a final volume of 50 µL. The assay components included a final LasB concentration of 0.3 nM and a substrate concentration of 150 µM. Compounds were incubated with the enzyme for 15 min at 37 °C before the addition of substrate. All experiments were performed in duplicate and included blank (no enzyme) controls. Additional controls included testing of other components, namely leucine and mannitol.

After blank subtraction, the slope of samples containing inhibitors (υ) was divided by the slope of simultaneously initiated uninhibited enzymatic reactions (υ_0). IC_{50} values were determined by non-linear regression analysis using GraphPad Prism 9 (Graph Pad Software, San Diego, CA, USA).

2.11. MMP inhibition assay

The MMP assay was performed using a commercially purchased Sensolyte 520 generic MMP assay kit (Anaspec, Fremont, CA, USA) according to the manufacturer's protocol. MMP-1 and MMP-2 were chosen from the potentially involved MMPs as illustrative and relevant for pulmonary fibrosis. A FRET-based inhibition assay utilized a substrate susceptible to MMP cleavage, releasing a fluorescent by-product that was quantified using a fluorimeter. This quantification provided a measure of the extent of inhibition. The assay involved an initial incubation of the formulation containing phytic acid, mannitol, and leucine with the respective MMP for 1 h at room temperature. The determination of the percentage of enzyme inhibition was calculated relative to the reference condition characterized by the absence of an inhibitor.

2.12. Cytotoxicity of formulation and active compound

The viability of A549 cells, a lung adenocarcinoma cell line, in response to formulated phytic acid or pure phytic acid was evaluated using the conversion of 3-(4,5-Dimethylthiazol-2-yl)−2,5-diphenyltetrazoliumbromid (MTT) to formazan (MTT assay). A549 cells were cultured in a 96-well plate at a seeding density of 10,000 cells per well and allowed to reach 80 % confluence for several days. Subsequently, different concentrations of phytic acid, ranging from 0 to 6000 µg/mL, were added in Hanks' Balanced Salt Solution (HBSS). The assay involved removal of the cell culture medium followed by two washing steps with HBSS pH 7.4. A positive control (HBSS + 1 % TritonX-100) and a negative control (HBSS alone, untreated cells) were added, and all samples were incubated at 37 °C for 4 h on an orbital shaker.

After incubation, the supernatant was aspirated and again washing with HBSS was performed. The cells were then incubated in 100 µL HBSS + 10 µL MTT (5 mg/mL PBS) for 4 h at 37 °C on a shaker. The resulting supernatant was removed and 100 µL DMSO was added, followed by incubation in the dark at 37 °C on a slow shaker for 10 to 30 min (dissolution of formazan crystals). Measurements were made using the Tecan i-control reader software at an absorbance of 550 nm.

3. Results and discussion

3.1. Formulation optimization

3.1.1. Solvent optimization for spraying process

Several parameters were investigated to improve the particle characteristics of the dry-powder formulation. A key aspect under investigation was the choice of solvent for dispersing the formulation. Three samples from different solvents were prepared, all with a 2 % solid fraction and spray dried at room temperature (20 °C). To judge the suitability of the solvent the samples were analyzed by laser diffraction (Malvern Mastersizer 2000).

Experimental configurations included formulations prepared with 50 % v/v acetone in water, 50 % v/v isopropanol in water and pure water. These organic solvents were selected for their potential to mitigate powder aggregation during the spray drying process as reducing the water content in the spray drying solution also reduces the residual moisture in the product (Sosnik and Seremeta, 2015). Furthermore, mixtures of water and suitable water-miscible organic solvents such as isopropanol and acetone could lower the final boiling point of the solvent system and allow spray drying at lower temperatures. Since phytic acid has a melting point below 25 °C, reducing the spray drying temperature was our first approach in reducing the tendency of agglomeration due to the aggregation state of the compound.

Interestingly, it was observed that the formulation consisting of 5 % phytic acid and 95 % mannitol in a 50 % acetone / water mixture exhibited the least favorable characteristics, as shown in Fig. 1 c. The presence of aggregates and agglomerates, manifested as the second peak in Fig. 1, is attributed to the comparatively suboptimal solubility of the formulation components prior to the initiation of the spray drying process.

Having a closer look on the graphs (Fig. 1) considering the volume-based particle size distributions (Table 2) confirms that the pure aqueous spray medium results in the formation of smaller particles with a narrower particle size distribution. This is evidenced by the lower volume-based mean value, D[4,3], and the low span value (Table 2). The isopropanol-water mixture exhibits inferior but relatively comparable outcomes, whereas the acetone-water mixture demonstrates significantly inferior results with regard to average size and size distribution. Both the volume-based mean value, D[4,3] and the span value exhibit pronounced larger values.

A comparison of the particle distribution by volume shows that the spray solution of pure water has the best particle distribution. The majority of the spray dried microparticles have a particle diameter of <3 µm, which is a positive indicator for pulmonary application (Table 2). Comparing the areas of the first peak of sample A and B, the peak area in sample A is larger (Fig. 1). Conversely, the peak area of the second peak is larger in sample B than in sample A. This means that sample B has fewer small particles (< 5 µm) and more large particles (> 10 µm) compared to sample A. This could be due to the more hydrophobic character of acetone compared to isopropanol. The initial hypothesis that reducing the water content by using organic solvents in the spray drying solution would reduce the residual moisture and thus the agglomeration of the particles could not be confirmed. Instead, the experiments revealed that the polarity of the solution has a much stronger influence on the size distribution. The solubility of D-mannitol in water at 20 °C is 157 mg per gram of solution. In contrast, for the mixture of water and acetone with a volume ratio of 1:1, the solubility at 20 °C is 34

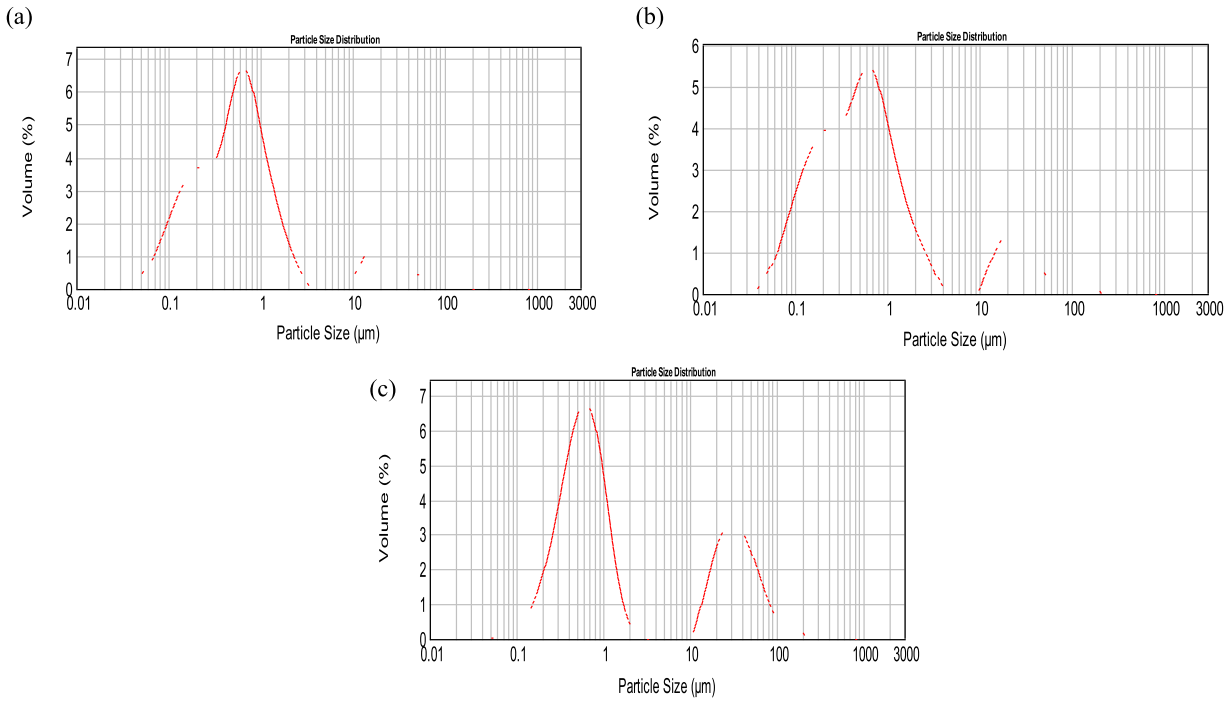

Fig. 1. Particle size distribution by volume% by laser diffraction. (a) 5 % phytic acid in 100 % water (b) 5 % phytic acid in 50 % isopropanol and 50 % water (c) 5 % phytic acid in 50 % acetone and 50 % water.

Table 2
Particle size distribution by volume%, (a) 5 % phytic acid in 100 % water (b) 5 % phytic acid in 50 % isopropanol and 50 % water (c) 5 % phytic acid in 50 % acetone and 50 % water.

Sample composition	D [4,3] (µm)	D10 (µm)	D50 (µm)	D90 (µm)	Span
(a) 5 % PA 95 % Man 100 % water	3.60	0.131	0.567	12.86	22.45
(b) 5 % PA 95 % Man 50 %isoprop-water	5.60	0.12	0.54	17.79	32.93
(c) 5 % PA 95 % Man 50 % acetone-water	14.62	0.23	0.79	5.08	63.57

mg per gram of solution medium (Cares-Pacheco et al., 2014). The polar phytic acid and especially mannitol were best spray dried from a polar solvent. In addition, the product yield of the aqueous spray solution was significantly higher compared to the mixtures with organic solvents which was obvious already by visual inspection. The spray drying products of the organic spray solutions stuck more in the drying chamber or in the cyclone of the spray dryer and could not be well collected.

The second reason for the decision to use water as spray drying medium is related to the possible residues of acetone or isopropanol, which might increase the cytotoxicity of the formulation. Therefore, water was used as solvent for the formulation in the upcoming experiments. However, a second smaller peak was always observed in the sprayed product due to undissolved larger crystals or aggregation due to the known hygroscopicity of phytic acid.

3.1.2. Excipient optimization

Besides the solvent, also the excipient used to form the particle matrix is of high relevance. Various common carrier materials and filling agents were used to adjust and to stabilize the size and shape of the microparticles. Since the carrier material naturally represents the largest proportion of the formulation in terms of mass, it has a significant influence on the storage stability and aerodynamic properties of the formulation. These factors depend primarily on the shape and size of the particles. The most commonly used excipients for spray drying in the literature are mannitol, maltodextrin, lactose, trehalose, and sucrose (Littringer et al., 2012). We decided to try a selection of these to see which was best suited for the formulation. Due to the high sticky tendency of phytic acid, which is transferred to the spray-drying product with increasing content, only a small mass fraction of 5 w% was utilized. In order to test the limits, up to 15 w% phytic acid was used in the case of mannitol. In the case of lactose with 5 % phytic acid, the powder in the cyclone was very sticky and produced poor results; there was only a very low product yield and thus lactose was discarded as excipient for the phytic acid formulation.

Subsequently, we considered the incorporation of trehalose, a non-reducing sugar, into the formulation. Samples with a phytic acid content of 5 % (w/w) were spray dried together with a trehalose matrix of 90 and 95 %, respectively. The solid fraction in the spray solution was 2 %. Unfortunately, these efforts did not yield positive results or product yield due to the sticky nature of the resulting powder. Thus, maltodextrin was explored as an alternative excipient. Known for its safety profile and ability to encapsulate a wide variety of active ingredients, maltodextrin is a carbohydrate commonly used as a thickening or bulking agent. Maltodextrin exists in several grades, which are classified based on their dextrose equivalent (DE), with a higher DE corresponding to shorter glucose chains (Ganaie et al., 2021).

Maltodextrin variants, specifically maltodextrin (4–7) and maltodextrin (16.5–19.5), have been introduced in combination with 5 % phytic acid. Unfortunately, these formulations also failed to produce good results evidenced by the lack of powder accumulation in the collection cup (Fig. 2).

In contrast, mannitol showed the highest product yield (around 12.15 %) of all the matrix excipients tested, even if this was still low. However, it was not possible to determine the exact yield, as the product stuck strongly to the glass of the cyclone, which can be seen in Fig. 2. The excipients maltodextrin, lactose, and trehalose showed larger agglomerates that were removed by the cyclone. In addition, these three compounds formed a very hard film on the inside of the cyclone that could not be collected. This is often the case when the product is still too moist

Fig. 2. Images for the cyclone with different drug-carriers with 5 % phytic acid. (a) Mannitol (b) Maltodextrin (16.5–19.5) (c) Lactose (d) Trehalose, after spray drying.

when it enters the cyclone. The usual solution is to increase the drying temperature, but since phytic acid has a melting point below 25 °C, we assumed that increasing the inlet temperature would lead to fluidization of the phytic acid, resulting in an increase in the tendency to stick or agglomerate.

The morphology of spray dried particles with different amounts of phytic acid were imaged by scanning electron microscopy (SEM) (Fig. 3). The 0 %, 5 %, 10 % and 15 % phytic acid with the selected excipient (mannitol) were examined to evaluate the applicable phytic acid content in the formulation; it was found that more agglomerates occur with increasing phytic acid content. This is expected as the phosphate groups can form hydrogen bonds and therefore more water remains in the particles. The formulation for each experiment was spray dried at room temperature (20 °C).

3.1.3. *Conversion of phytic acid to sodium phytate*

The challenge was therefore that the stickiness or agglomeration tendency increased for two reasons when the phytic acid content increased: The first reason is obviously the hygroscopicity of phytic acid. The six phosphate groups interact *via* hydrogen bonds with the surrounding humidity, as shown in Fig. 4.

Hygroscopicity can be a problem with dry powders for inhalation therapy, as it is the main cause for aggregation of the particles in the formulation and thus impairs the aerodynamic properties. Mannitol is a sugar alcohol that has been shown to be non-hygroscopic and is even used specifically to protect hygroscopic drugs (Ng et al., 2022). In addition, the absorption of moisture can affect the contamination risk of the formulation as it provides a good environment for microbial growth.

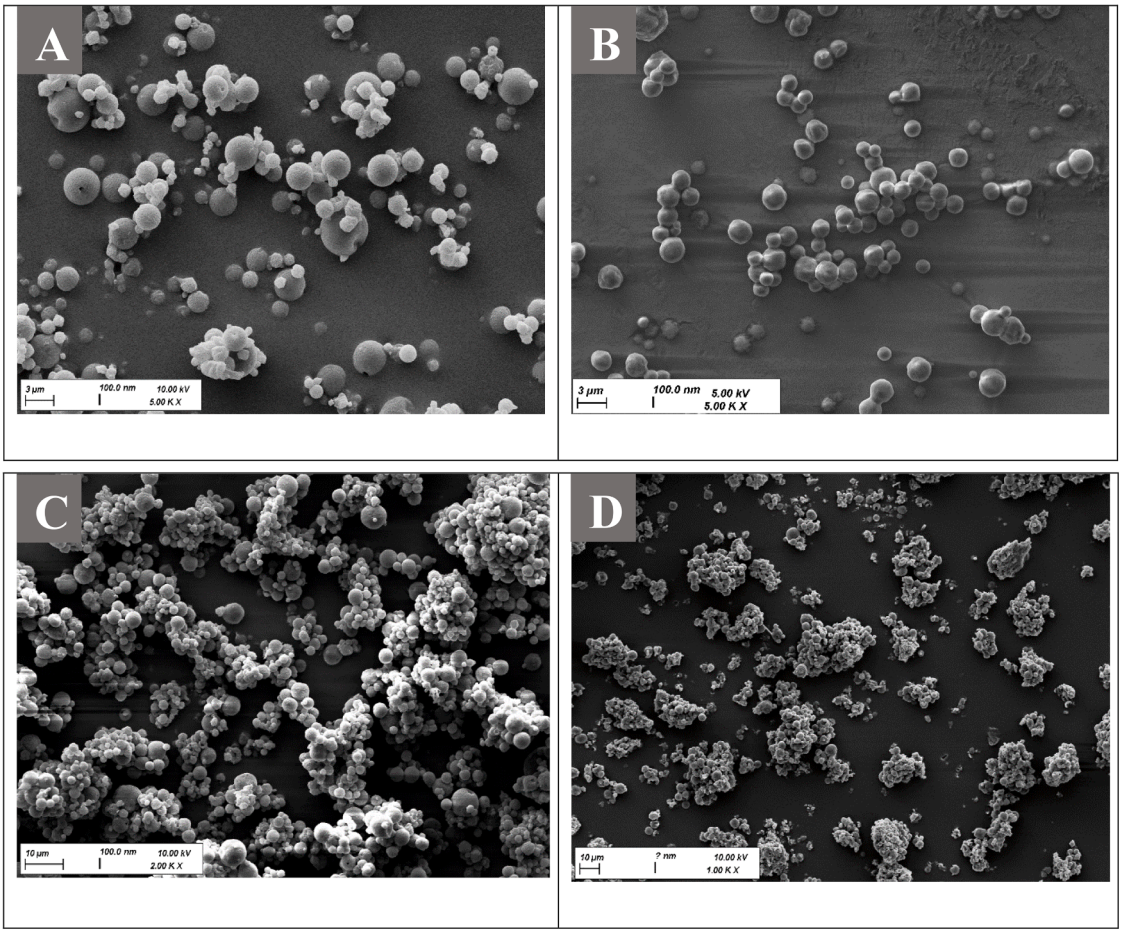

Fig. 3. Morphology analysis by using the scanning electron microscope (SEM); the samples differ in the content of the phytic acid. (A) 0 % phytic acid (B) 5 % phytic acid (C) 10 % phytic acid (C) 15 % phytic acid.

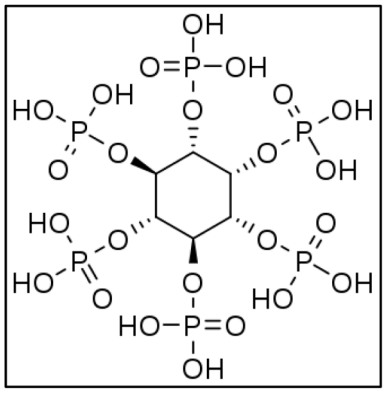

Fig. 4. Structure of phytic acid (PA), also known as inositol phosphate 6 (IP-6); showing 6 phosphate groups and 12 exchangeable protons (*H*+).

Furthermore, aggregation of the powder can interfere with drug release and clog the delivery device, resulting in reduced delivery efficiency and further compromising patient compliance. The second reason for agglomeration is the low melting point of phytic acid, which is below 25 °C (CAS_Common_Chemistry, retrieved 2024-02–23). The melting point has a major impact on the spray drying process.

Spray drying was performed at room temperature (20 °C) around the melting point of phytic acid. Fractions of the phytic acid will therefore be in a liquid state during the spray drying process. Mannitol can compensate for a certain part of the negative phytic acid properties. However, if the phytic acid content is too high, the microparticles stick together and form larger agglomerates within a short time, which cannot be dispersed.

The challenges associated with formulating a stable co-amorphous blend can potentially be overcome by using a salt form of phytic acid. The salt form offers several advantages, including improved product stability and solubility, and reduced hygroscopicity (Korn and Balbach, 2014). The salt form contributes to improved physical properties of the resulting powder, leading to improved handling, thereby mitigating issues such as particle aggregation.

There are two different methods for obtaining the salt form of phytic acid: using sodium phytate as a commercially available powder or adding a strong base, such as sodium hydroxide, to phytic acid to convert it to the salt form. The latter option is superior because it allows the pH of the formulation to be adjusted to the physiological level of 7.4 while at the same time converting phytic acid to sodium phytate salt.

Phytic acid, also known as inositol phosphate 6 (IP6), is known to contain twelve exchangeable protons within its six phosphate groups. The *pKa* values for these protons have been previously approximated (Costello et al., 1976), highlighting six highly acidic protons (*pKa* 1.5), 3 weakly acidic protons (*pKa* 5.7 - 7.6), and the remaining three protons possessing a *pKa* >10. It is estimated that at pH 7.4, phytic acid assumes a configuration with eight sodium ions. The molecular weight of Na8PA can be calculated as (PA MWT) + (8Na MWT) – (8H MWT) = 660.04 + 183.84 – 8.05 = 835.83 g mol^{-1} (Costello et al., 1976).

3.1.4. Investigation of increasing the inlet temperature

Two spray drying tests were performed, each with a phytic acid content of 15 %. One sample was spray dried at an inlet temperature of 66 °C and the other at room temperature (20 °C), i.e. without active heating of the drying air. The two samples were examined using SEM to observe the effects of heat on the formulation and its morphology (Fig. 5).

The thermal energy introduced into the system has a significant effect on the properties of the particles produced by affecting the evaporation rate leading to smaller particle sizes mainly due to reduced water content. In this instance, we have a special case due to the use of phytic acid. Because of the very low melting point (< 25 °C), phytic acid is possibly molten, as we can only estimate the exact temperature of the particles during the process approximately via the outlet temperature (51 °C). Although an improvement can be seen when comparing Fig. 5 a and b, the liquid phytic acid causes the agglomeration of the particles in Fig. 5 b. In addition to adjusting the inlet temperature, other parameters must therefore be optimized. One possibility would be the salt formation of the phytic acid with sodium hydroxide solution. The melting point of sodium phytate is determined by the bound crystal water and is approximately 58 °C (Pedersen et al., 1953). This temperature is higher than that of pure phytic acid (< 25 °C), which means that the melting point of sodium phytate is not reached, resulting in the formation of fewer agglomerates.

3.1.5. Investigation of the leucine influence

Leucine is well-known as an efficient adjuvant in spray drying, which can improve the microparticle properties in several ways (Alhajj et al., 2021). To investigate the influence of leucine on the aggregation tendency of the particles, a 15 % phytic acid sample with different leucine contents was spray dried. Due to its amphiphilic structure, which is due to its hydrophobic and hydrophilic part, it concentrates on the shell of the evaporating dispersion droplet, forming a leucine shell around the microparticles at the end of the spray drying process (Li et al., 2016).

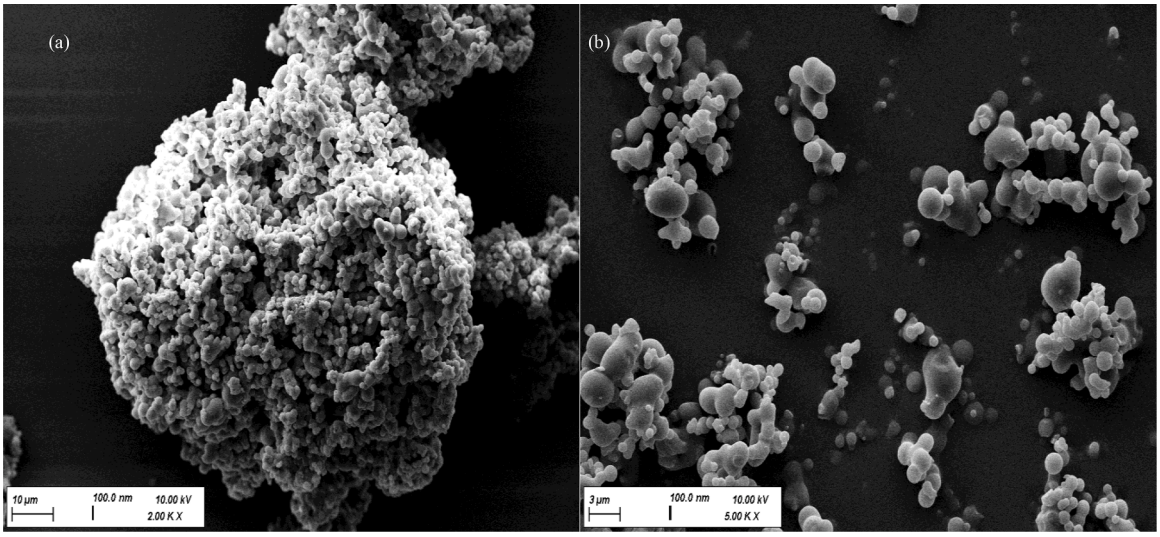

Fig. 5. SEM images showing the heating effect differences (a) 15 % phytic acid pH: 7.4, inlet temperature: RT (b) 15 % phytic acid pH: 7.4, inlet temperature: 66 °C.

This is the reason why leucine is known to improve the dispersibility, to act as an anti-caking agent, to improve storage stability, to reduce particle hygroscopicity and to improve aerodynamic properties, such as increasing the fine particle fraction (FPF) of the formulation (Mah et al., 2019).

In Fig. 6(a), the particles are close together but are not agglomerated. The microparticles in Fig. 6(a) have a spherical structure with a smooth corrugated surface. It is known that L-leucine accumulates on the droplet surface during spray drying, forming a hydrophobic crystalline outer shell that changes the surface morphology and reduces the interparticle cohesive forces (Alhajj et al., 2021). The leucine-free sample in Fig. 6(b) also shows spherical particles with sizes ranging from 1 to 3 μm. However, these particles form larger particle agglomerates of about 10-15 μm. The fact that the particles are more separated by using L-leucine confirms that the hygroscopic property of phytic acid leads to more agglomerates. This agglomeration-prone property is successfully compensated by a 10 % L-leucine content. Due to the use of 10 % L-leucine, the particles now have a rougher surface. Nevertheless, only a few particles look raisin-shaped, and a few particles also look imploded. This is a typical structure caused by the collapse of the L-leucine shell. The leucine shell encloses the two more hydrophilic components mannitol and phytic acid. As a result, phytic acid is shielded from the moisture in the air. As a result, microparticles are formed whose agglomeration tendency decreases since the leucine has formed an outer protective barrier.

As shown in Fig. 7, leucine contents of 5 %, 10 %, 20 % and 35 % were analyzed as a powder using laser diffraction (HORIBA Partica LA 950). Particle dispersion in air was achieved by the application of an air stream. The phytic acid content was maintained at 15 % for all samples, with the remaining matrix consisting of mannitol and leucin.

The particle size distribution (Fig. 7) shows that the microparticles of all produced samples are mostly in a range between 1-10 μm. The distribution is a more or less symmetric peak without a second particle collective as found before (Fig. 1).

A closer look at the statistical parameters of the particle size distribution confirms the positive result of the size measurements. If we first compare the average and median particle sizes with each other, this value is, as expected, highest for the sample with the lowest L-leucine content of 5 % (w/w) at 4.36 μm and 4.38 μm, respectively.

Due to its amphiphilic structure, L-leucine has surface-active properties that reduce the surface tension of the sprayed droplets. This results in the formation of smaller droplets when the active-ingredient solution is atomized, which, in turn, results in smaller microparticles (Alhajj et al., 2021). Furthermore, L-leucine reduces the interparticle cohesive forces by forming a hydrophobic shell (Alhajj et al., 2021). This leads to fewer microparticle agglomerates, which also reduces the median and mean particle diameter, see Table 3. If we now compare the D90 value of the different samples, this is also highest for the first sample (5 % L-leucine). This is in line with the previous results, as it means that about 10 % of the particles are larger than 10 μm. This could be an indication of agglomeration, although this only took place to a very small extent. A 5 % L-leucine content could therefore be considered insufficient. Finally, if we look at the Span value, which indicates the width of the particle size distribution, this is greatest for the 5 % L-leucine sample at 1.82. This means that the particle size distribution is wider than in the other samples. As the L-leucine content increases, this value decreases relatively sharply. The above-mentioned reduction in the agglomeration tendency also increases the uniformity of the particle size distribution. The narrower particle size distribution can also be seen in Fig. 7. With a median particle diameter between 3.24 and 4.38 μm, the majority of the spray dried particles should also be able to reach the deepest areas of the lung, such as the bronchial and alveolar regions (Carvalho et al., 2011). Finally, it should be noted that the average and median particle diameters of each sample are very close to each other. This confirms a relatively symmetrical particle distribution (Fig. 7) and confirms the absence of many small agglomerates or few very large agglomerates, as otherwise the mean diameter would deviate upwards from the median value.

3.1.6. Optimization of the procedure considering the phytic acid content

After adjusting the mannitol and leucine concentrations, it is imperative to systematically vary the phytic acid content to ensure sustained optimization of aerodynamic properties within the formulation, especially as phytic acid levels increase. For this, the leucine content was kept constant at 20 %. Experimental evaluations included testing various levels of phytic acid from 10 % to 40 % and determining the particle sizes after spray drying.

Both median mass aerodynamic diameter (MMAD) and fine particle fraction (FPF) are key parameters in describing the aerodynamic characteristics of a substance. The MMAD, which represents the median diameter at which half of the particle mass is below and half is above, helps to characterize particle aerodynamics and deposition profiles in the lung. The geometric standard deviation (GSD) indicates the width of the particle size distribution. The smaller the GSD, the narrower the size

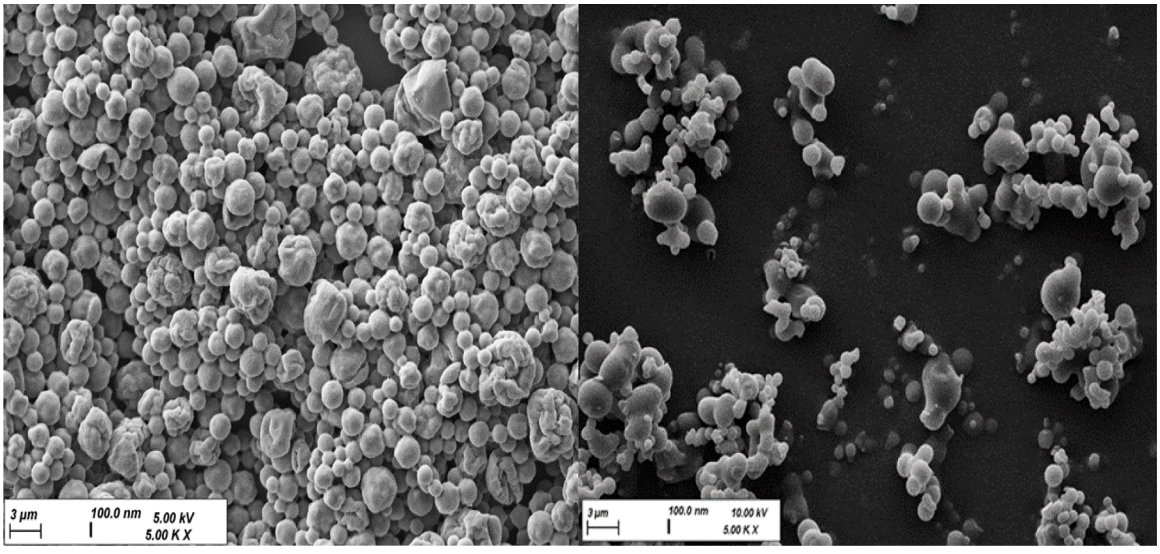

Fig. 6. SEM images showing the leucine effect differences (a) 15 % phytic acid + 10 % leucine, inlet temperature: 66 °C (b) 15 % phytic acid, inlet temperature: 66 °C.

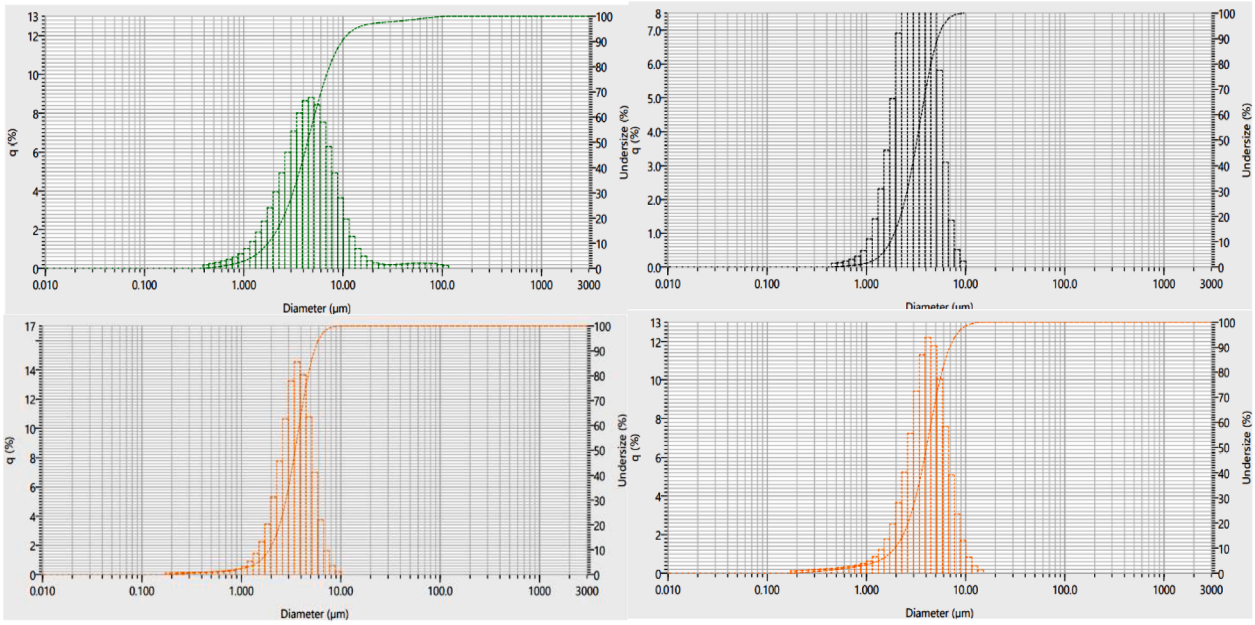

Fig. 7. Volume based particle size distributions of formulations of different leucine content measured by laser diffraction (on the HORIBA Partica). (a) 5 % leucine (b) 10 % leucine (c) 20 % leucine (d) 35 % leucine. (a) shows some aggregates in the range of 10 – 100 µm. (b), (c) and (d) show relatively lower dispersity (10 and 20 % leucin show the lowest SPAN values followed by the formulation with 35 % leucin.

Table 3
Volume based particle size distribution of formulations (66 °C inlet) with different leucine content (5 %, 10 %, 20 % and 35 %), a constant amount of phytic acid (30 %) and a variable amount of mannitol.

Sample composition	D [4,3] (µm)	D10 (µm)	D50 (µm)	D90 (µm)	Span
30 % PA 5 % L-leucine 65 % mannitol	4.36	1.76	4.38	9.76	1.82
30 % PA 10 % L-leucine 60 % mannitol	3.11	1.76	3.24	5.24	1.08
30 % PA 20 % L-leucine 50 % mannitol	3.27	1.91	3.48	5.45	1.02
30 % PA 35 % L-leucine 35 % mannitol	3.73	1.94	4.03	6.94	1.24

distribution. This is crucial for targeted and thus localized deposition in the lungs. In order to reach the bronchial and alveolar areas of the lung, the particles should be smaller than 3 µm (Carvalho et al., 2011). A GSD < 1.15 is a monodisperse particle collective, which is difficult to achieve in reality. Therapeutical formulations often show GSD values around 2.0 (Voshaar, 2005).

This knowledge helps improve the design of inhaler powders for localized drug delivery. Conversely, FPF quantifies the fraction of particles considered "fine", including microparticles smaller than 5 µm that can reach the deepest lung compartment (Buttini et al., 2013). The emitted dose (ED) is the amount of a drug that is actually released from a delivery device, such as an inhaler or nebulizer, and is available for patient inhalation (Buttini et al., 2013). It was expressed as a percentage of the total dose per capsule.

Table 4 shows that phytic acid concentrations of 10 %, 20 % and 30 % gave satisfactory results in terms of MMAD and FPF. However, with an MMAD larger than 5 µm and a fine particle content of only 28.48%, the 40 % phytic acid sample does not have optimal aerodynamic properties to reach the deep areas of the lungs. A large proportion of this sample would be deposited in the extrathoracic area of the lungs or already in the mouth/pharynx (Artmann and Staudinger, 2021).

Table 4
Aerodynamic properties for various formulations with 10 %, 20 %, 30 % and 40 % phytic acid and constant amounts of leucine (20 %). Data was generated using the Next Generation Impactor (NGI).

Sample composition	MMAD (µm)	GSD	FPF (%)	ED (%)
10 %PA, 20 % leucine, 70 % mannitol	2.67	2.56	56.29	88.11
20 %PA, 20 % leucine, 60 % mannitol	2.74	2.38	61.01	82.74
30 %PA, 20 % leucine, 50 % mannitol	3.52	1.62	61.52	78.43
40 %PA, 20 % leucine, 40 % mannitol	5.79	2.04	28.48	69.11

The remaining samples have an MMAD close to 3 µm and should therefore be able to reach deep-lung sections. The GSD of all samples is around 2, which indicates a size distribution in accordance with typical formulations (Voshaar, 2005). The most important parameter is the FPF, which looks very good for the first three samples (Table 4) with a value of around 60 %. The data on the emitted dose (ED) demonstrate a trend. As the phytic acid content increases, the ED decreases, thereby reducing the available dose for inhalation. Besides the aerodynamic properties the delivered dose is a key parameter, which puts the formulation with 30 % phytic acid in focus as a good choice.

The application of heat proved to be a key parameter essential for the successful execution of the spray drying process. An optimum inlet temperature of 66 °C was identified in a set of temperature-related experiments. This inlet temperature resulted in a corresponding outlet temperature of 51 °C. In conclusion, spray drying of phytic acid presented initial challenges due to its hygroscopic nature and a melting point of 25 °C. However, these challenges were overcome by careful formulation optimization, incorporation of appropriate excipients such as mannitol, and addition of leucine as an additive to improve dispersibility.

The use of L-leucine as a spray drying aid in the formulation played a crucial role in improving both the physical and functional properties of the resulting product. This enhancement manifested in improved storage stability, increased flowability, and a reduction in stickiness, as elucidated by Li et al. (2016). The strategic introduction of additives effectively mitigated the inherent challenges associated with the spray drying of phytic acid. In addition, changing the pH of the solution prior to spray drying, from a highly acidic state (pH 2.3) to a physiological pH (7.4), proved to be of paramount importance. This adjustment not only made the formulation suitable for inhalation into the lungs, but also induced a chemical conversion of phytic acid to sodium phytate.

Table 5
Moisture content of the spray-dried formulations.

Sample composition	Moisture content (%)
10 %PA, 20 % leucine, 70 % mannitol	2.52
20 %PA, 20 % leucine, 60 % mannitol	2.64
30 %PA, 20 % leucine, 50 % mannitol	4.13
40 %PA, 20 % leucine, 40 % mannitol	7.46

3.1.7. Moisture content of the spray-dried formulations

Table 5 shows the moisture content of the spray-dried formulations containing different concentrations of mannitol (40 - 70 %), measured via thermogravimetric analysis, by infra-red drying at 130 °C. Thermogravimetry determines the loss of mass that occurs when the sample is heated (Ohrem et al., 2014). From the table we can see that the sample with the highest mannitol amount showed a lower moisture content compared to the other samples. This could be explained by the physicochemical properties of mannitol, such as the low hygroscopicity. A higher amount of mannitol in the formulation might protect the powder from adsorbing moisture from the environment (Ohrem et al., 2014). However, we can conclude from the values that in general, for all the formulations the moisture content is low (Sartorius_AG, 2018).

3.1.8. Characterization of the final formulation

A final formulation of 30 % phytic acid, 20 % leucine, and 50 % mannitol was selected based on the results of both the Next Generation Impactor (NGI) and the HORIBA Partica. The median particle size determined by the HORIBA Partica was recorded at 3.48 μm using laser-scattering and image analysis in a dry chamber for particle size measurement, as shown in Table 3.

Simultaneously, the identical formulation was tested with the Next Generation Impactor (NGI) to ensure aerodynamic properties, resulting in a MMAD of 3.52 μm and a FPF of 61.52 %, as detailed in Table 4.

The next step was to test the final formulation for storage stability, as it is important to ensure that the dry-powder formulation does not degrade over the storage period. For this purpose, the formulation was stored in a desiccator for 40 days. Fig. 8a shows the formulation after production. Except for a few agglomerates, the particles appear separate and distinct. The particles have a spherical appearance and a diameter of approximately 13 μm. After ten days, the particles in Fig. 8b are still separated and intact. The shape of the particles has not changed. After 40 days of storage, the particles in Fig. 8c appear highly agglomerated. In some cases, no interparticle spaces are visible because the particles are connected by visible solid bridges.

As mannitol and L-leucine have no hygroscopic properties (Sou et al., 2016) phytic acid with its strong hydrophilic properties due to the six phosphate groups attracts environmental water. This effect was greatly reduced by transformation into sodium salt (Costes et al., 2015), but sodium phytate is still hygroscopic. The amorphous structure of spray dried products makes them susceptible to absorbing moisture from the air. Mannitol, which forms the matrix and the largest component by mass, cannot compensate for this effect with its non-hygroscopic properties. The L-leucine also does not seem to be able to protect the particles sufficiently over the 40-day storage period. Therefore, it can be assumed that the formulation needs to be further optimized. This can be done either by reducing the amount of active ingredients or by increasing the amount of L-leucine. Another possibility would be packaging optimization, such as the use of moisture-absorbing or moisture-repellent barriers.

Moreover, we performed XRD analysis on the final formulation directly upon spray drying and after being stored for more than a year in the desiccator. The XRD spectra show that the spray-dried PA formulations are crystalline (Supplementary information, Fig. S2). We assume that crystallinity comes due to the presence and interaction of mannitol and leucine in the formulation, as phytic acid itself is not crystalline. In addition, we could observe no difference between the XRD spectra of the freshly prepared powder, and the powder stored for more than a year.

3.2. Chemical and biological assays

3.2.1. Zinc-Phytic acid chelation validation

Our hypothesis was based on the premise that chelation of phytic acid with Zn^{2+} leads to inhibition of Zn^{2+}- dependent protease enzymes that are critical for tissue remodeling. To validate this proposed mode of action, chelation was assessed using a fluorometric assay. The kit contains a probe whose fluorescence is enhanced exclusively upon interaction with Zn^{2+} ions. As shown in Fig. 9, phytic acid demonstrated a remarkable chelating capacity (CC), as indicated by its low CC_{50}, the concentration at which 50 % of Zn^{2+} was chelated. The CC_{50} for pure phytic acid was measured to be 6.381 μM and for the formulated phytic acid it was 5.403 μM. Given that the amount of Zn^{2+} added was 8.5 μM, the comparable values between the Zn^{2+} added and the CC_{50} values for both pure and formulated phytic acid underscore the efficacy of phytic acid as a zinc chelator.

Furthermore, the nearly equivalent values of the CC_{50} for formulated and pure phytic acid suggests stability of phytic acid for the temperatures used during the spray drying process.

3.2.2. Simulating the molecular zinc ion chelation

To complement the empirical investigation, a molecular dynamics (MD) simulation using the Molecular Operating Environment (MOE) was performed, focusing on two phytic acid molecules interacting with eight Zn^{2+} ions (Fig. 10). At a neutral pH, phytic acid is eight times deprotonated and negatively charged (Costello et al., 1976). This charge can be compensated by 4 Zn^{2+}- ions. Due to the large number of reactive phosphate groups, phytic acid can form a complex with a cation within a phosphate group itself, between two phosphate groups of a molecule, or

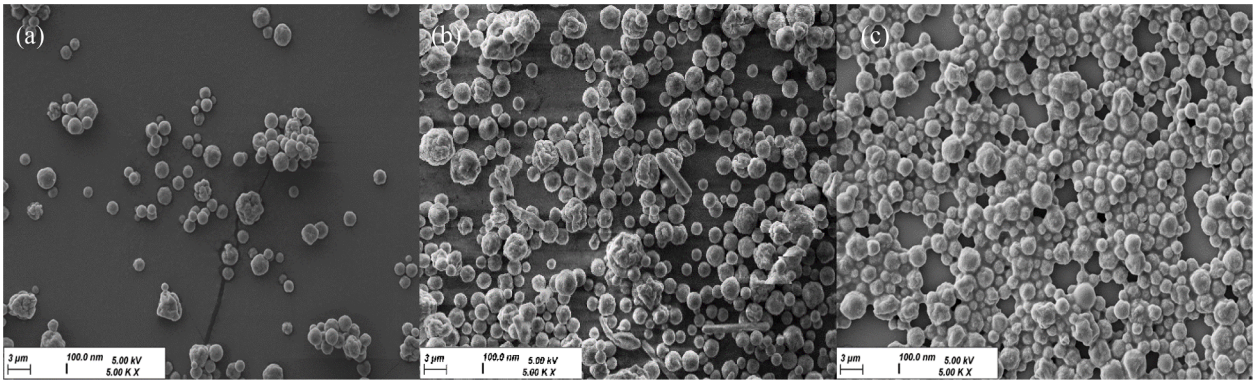

Fig. 8. SEM images of the final formulation over different storage times (30 % phytic acid, 20 % leucine, and 50 % mannitol) stored in the desiccator for (a) 0 days, (b) 10 days, and (c) 40 days.

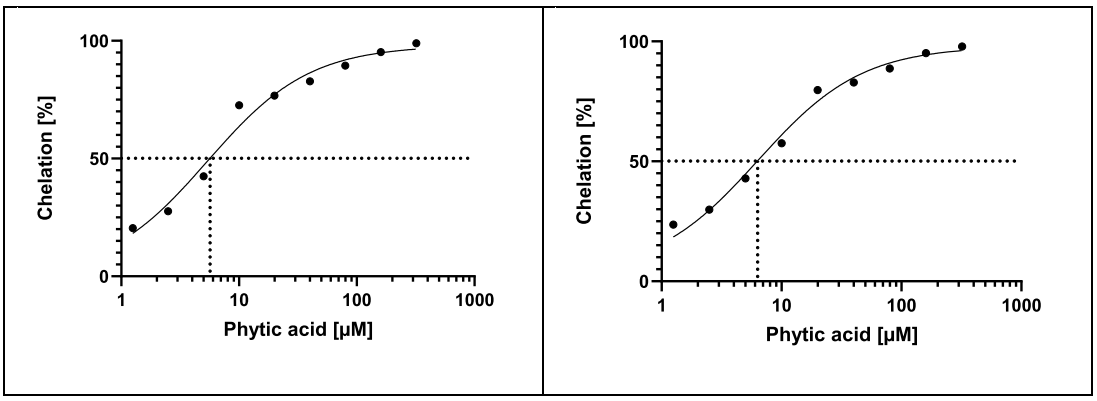

Fig. 9. Percent chelation plot of phytic acid with 8.5 µM of Zn^{2+} (left) formulated phytic acid (right) pure phytic acid.

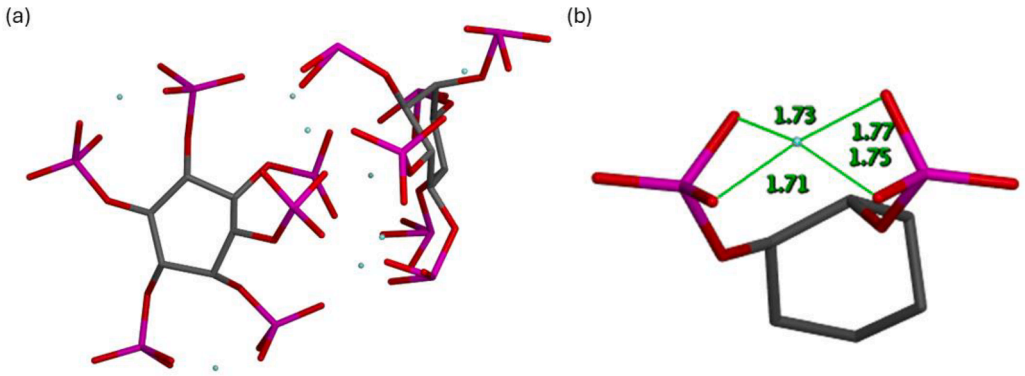

Fig. 10. MOE simulation of 2 phytic acid molecules with eight Zn^{2+} ions (light blue) (a) The found best conformer of the chelated Zn^{2+} with phytic acid (b) Zoom in on one of the Zn^{2+} ions chelated with the oxygen atoms, in green is the distance between the Zn^{2+} and oxygen atoms in angstroms.

between phosphate groups of different phytic acid molecules (Gosselin and Coghlan, 1953). It cannot be assumed that there is only one fixed constellation between zinc ions and phytic acid. Therefore, the simulated zinc ion chelation here is only one possible chelation constellation.

The simulation elucidated that oxygen moieties play a key role in the chelation process, with a Zn^{2+} ion likely coordinating through different segments of different phytic acid molecules. The interaction is assumed to be proximal, given the approximate distance of 1.7 Å between the O^{2-} and the Zn^{2+}. In literature typical bond lengths between Zn^{2+} and O^{2-} are between 1.8 and 2 Å with 4 coordination bonds (Gagne and Hawthorne, 2020). The distances between H_2O and Zn^{2+} are described to be around 2 Å (Cauet et al., 2010). As the bond strength correlates with the distance between the binding partners (Badger, 1934), the chelation in our case is tight and seems to be stronger.

3.2.3. *Assessing LasB inhibition of the formulation*

The successful identification of the complexation potential of phytic acid for zinc ions is one step on the way for a functional formulation. Besides this, the biological activity is a key parameter. The intended biological effect of the final formulation and pure phytic acid was evaluated using a functional LasB inhibition assay. Evaluation of both the formulated product and pure phytic acid against the bacterial protease enzyme LasB produced by *P. aeruginosa* was essential to gain insight into the potential antivirulence activity of the tested formulation.

The LasB assay was performed with pure PA and with the final formulation also containing L-leucin and mannitol. The IC_{50} of pure phytic acid was 121.2 µg/mL and the IC_{50} of formulated phytic acid was 109.7 µg/mL (Fig. 11), which is equivalent to 362 µg/mL of the total formulation including phytic acid and the excipients. In addition, mannitol and leucine were shown to have no inhibitory activity at a

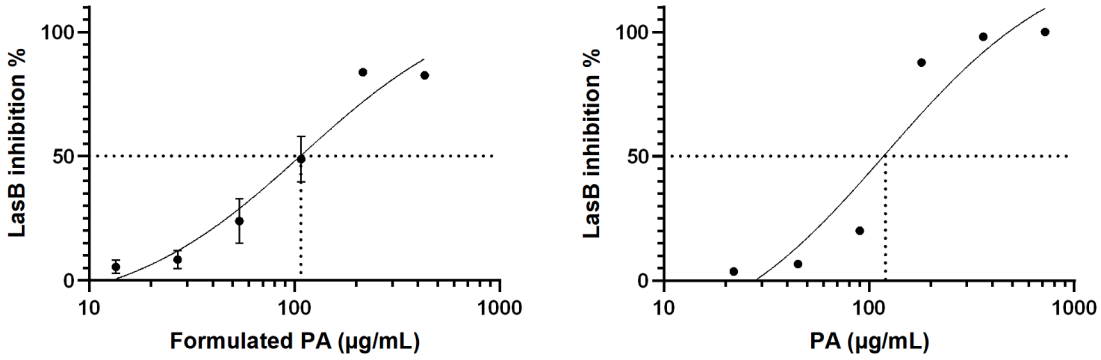

Fig. 11. Inhibitory activity of (a) formulated phytic acid ($n = 2$) and (b) pure neutralized PA on the bacterial metalloprotease LasB.

respective concentrations of 1293 μg/mL (due to solubility limitations) when used alone. Literature research revealed that the IC_{50} of phytic acid determined for LasB was 10 to 20-fold less efficient than those reported for some other LasB inhibiting compounds (Konstantinovic et al., 2023).

The IC_{50} values obtained of 110–116 μg/mL were not cytotoxic to the alveolar cell line A549, showing 82–100 % viability at this concentration, depending on whether the formulation contained formulated or pure phytic acid. In summary, phytic acid acts by chelating the Zn^{2+} ion, thereby successfully inhibiting LasB activity. The inhibition of this mechanism contributes to the mitigation of *P. aeruginosa*-induced lung fibrosis, as highlighted in the relevant literature (Faraji et al., 2016; Saint-Criq et al., 2018).

3.2.4. Assessing the formulation for the inhibition of mammalian metalloproteases

Both pure and formulated phytic acid were tested against two MMPs, specifically MMP-1 and MMP-2. It was hypothesized that LasB inhibition would result in concomitant MMP inhibition. However, as shown in Fig. 12, the IC_{50} for MMP-1 and MMP-2 proved unattainable ($IC_{50} > 724$ μg/mL). The concentrations tested were constrained by the solubility limits of the formulation stock solution in water, which precluded testing at higher concentrations. In addition, formulated phytic acid exhibited turbidity at concentrations above 90 μg/mL due to an interaction between the phytic acid and the assay buffer (SensoLyte kit).

The results suggest a potential selectivity of phytic acid as an inhibitor of LasB in the context of pulmonary fibrosis-related infections, with limited inhibition of human MMPs – an aspect that may be advantageous looking at the inhibition of *P. aeruginosa* affected fibrotic action. However, the solubility challenge associated with phytic acid necessitates the implementation of an alternative method using a specific phytic acid compatible buffer to validate the observed minimal inhibition of MMPs. It should be noted that the LasB assay buffer contains a detergent, which may have contributed to the increased solubility of both pure and formulated phytic acid.

3.2.5. Assessing the cytotoxicity of pure and formulated phytic acid

The cytotoxicity of both the formulation and pure phytic acid was assessed using the MTT assay, as illustrated in Fig. 13. A549 cells, as model cell line for the deep lung, were subjected to incubation with concentrations ranging from 0 to 6000 μg/mL. Notably, nearly all concentrations of phytic acid exhibited low toxicity. In contrast, the formulated phytic acid demonstrated toxicity for values larger than 750 μg/mL, potentially attributed to the toxic effects of mannitol or leucine at higher concentrations. One reason could be osmotic stress, as mannitol is a well-known hyperosmolar osmolyte and is not metabolized by human cells. If the osmolarity is exceeded, this can lead to osmotic stress and affect the viability of A549 cells (Ortiz et al., 2022). Testing the cytotoxicity of the excipients reveals that mannitol does not induce cytotoxicity even at higher concentrations (Fig. S1). In contrast, we could observe reduction of cell viability when higher concentrations of leucin were applied (Fig. S1). According to the literature, a cytotoxic effect of L-leucine is not expected as leucine is an essential amino acid. However, the low solubility of leucin might contribute to the cytotoxicity at high concentrations, as it might cause a layer covering the cells and thus impact and increase the deposited concentration on the cells. The viability values suggest a safe application of the formulated phytic acid with respect to the inhibition of LasB which was found to be 109.7 μg/mL.

3.2.6. Considerations on the dosing regimen of phytic acid-based inhalation therapy

Looking at a potential application the question arises which doses need to be delivered and is this feasible for our inhalation approach. Kamp et al. reported that the administration of 330 μg of phytic acid by intratracheal instillation in rats was effective in reducing asbestos-induced fibrosis (Kamp et al., 1995). Comparing lung surfaces between rats and humans might be a straightforward approach to transfer

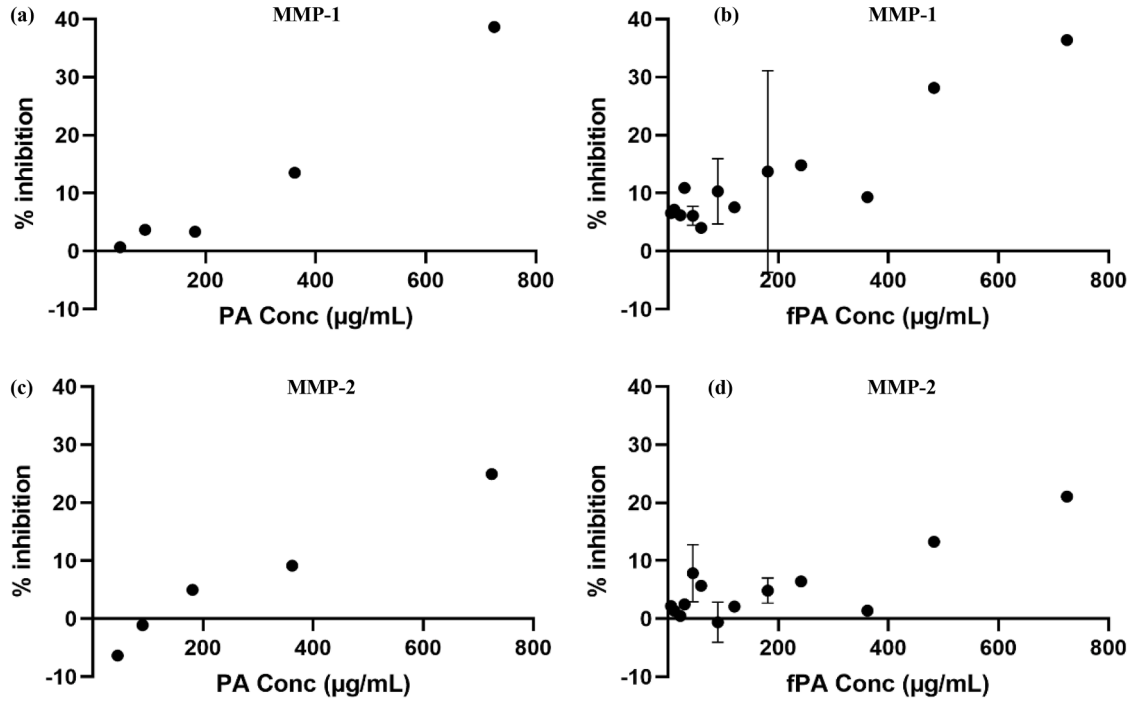

Fig. 12. % inhibition of MMP-1 and MMP-2 by pure and formulated phytic acid. (a) Pure neutralized phytic acid inhibition of MMP-1 (b) Formulated phytic acid inhibition of MMP-1 (c) Pure neutralized phytic acid against MMP-2 (d) Formulated phytic acid inhibition.

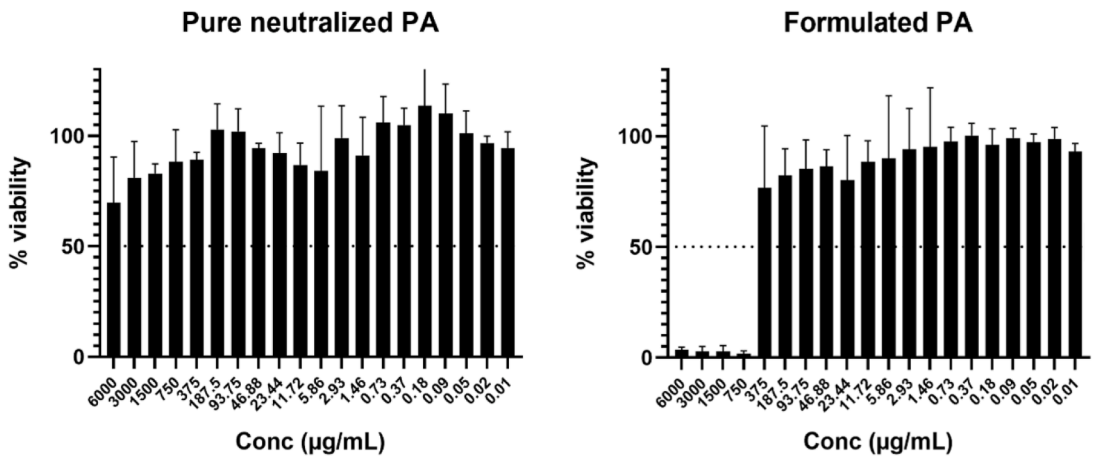

Fig. 13. Evaluation of cell viability after exposition of different phytic acid concentrations to A549 using MTT assay. (a) pH-adjusted pure phytic acid, (b) formulated phytic acid also containing mannitol and L-leucin displaying the concentration of the formulation used.

the respective drug amount. The human lung surface area is 250 times greater than that of SprageDawley rats (Nielsen and Koponen, 2018) resulting in a local delivery of 82.5 mg/day of phytic acid to the lungs as calculated from the following equation:

$$\textit{Amount in humans}\ (mg) = \frac{\textit{Amount in rats}\ (\mu g) \times \textit{Lung surface area}_{humans}/\textit{Lung surface area}_{rats}}{1000}$$

With respect to the anticipated effect on MMPs, Kapral et al. found a concentration of 660 µg/mL of phytic acid reducing mRNA copies of MMP-2, also an important contributor to fibrosis, in Caco-2 cells (Kapral et al., 2012). Considering the reported volume of the lining fluid in the lung (LFL) of 19 mL (Fröhlich et al., 2016), these concentrations correspond to a required dose of 12.54 mg (660 µg/mL phytic acid) and 2.2 mg for our case of the LasB inhibition (121.2 µg/mL), respectively, to reach these values in the human lung using the provided equation.

$$\textit{Amount}\ (\mathrm{mg}) = \frac{\textit{Volume of fluid in lungs}\ (mL) \times \textit{Concentration}\ (\mu g/mL)}{1000}$$

While the half-life of phytic acid in the lung is unknown, typical drug half-lives range from 0.5 to 3 h based on their properties (Himstedt et al., 2020). A rational approach to estimating the dosing regimen is to assume $\tau = t_{0.5}$, which represents half-life dosing. This implies that the drug concentration is maintained between the initial dose and 0.5 times the initial dose. Consequently, human dosing would require 8 to 48 doses per day to maintain more than half of the initial drug concentration. This corresponds to 100– 602 mg/day for the Caco-2 *in vitro* data and 18–106 mg/day for the LasB inhibition data using the provided equation:

$$\textit{Amount of drug}\left(\frac{mg}{day}\right) = \textit{One dose}\ (mg) \times \frac{24\ (\textit{hours})}{\textit{Half life}\ (\textit{hours})}$$

In this study, we estimated the required daily doses of 18, 82.5 and 110 mg to treat lung fibrosis.

However, it is important to recognize that the lung physiology of people with pulmonary fibrosis (PF) is significantly different from that of healthy individuals. The lungs of PF patients exhibit a distinctive pharmacokinetic profile characterized by a 3.5-fold reduction in intrapulmonary fluid volume (Rundfeldt et al., 2013). This reduction consequently reduces the total local volume of distribution. Furthermore, PF-affected lungs often exhibit prolonged drug half-lives ranging from 4 to 25 h, an eightfold increase compared to the normative pulmonary environment (Harvey et al., 2011; Ratjen et al., 2006). Adjusting our estimates in accordance with these considerations yields revised doses of 0.64, 3, 3.6, 3.8 and 21.5 mg/day for phytic acid, or 2.1, 10, 12, 12.7 and 71.7 mg/day for dry powder formulations containing 30 % phytic acid. This was assuming that the clearance is always eight times slower and correcting for the changed available pulmonary fluid (division by 3.5). Considering the results from the measurements of the aerodynamic properties revealed a maximum fine particle fraction of 61.4 %. Consequently, this would lead to a larger dose to be inhaled to reach the final doses up to 35 mg/day for pure phytic acid and 117 mg/day for the formulated phytic acid. These estimated doses might be in general feasible for targeted delivery to the human lung in powder form although the maximum values might be challenging.

In terms of toxicity, there are no documented cases of systemic toxicity associated with phytic acid. In terms of local toxicity, our results indicate a 50 % toxicity for >6 mg/mL for pure phytic acid on A549 lung cells–- a concentration significantly higher than those previously discussed. However, when phytic acid is combined with mannitol and leucine, we observe toxicity at 360 µg/mL for the formulated phytic acid, which is mainly attributed to the presence of leucine. It is noteworthy that optimization strategies can be pursued in the future to mitigate the observed toxicity if the required dose necessitates such adjustments.

Obviously, many assumptions underlie our preliminary assessment of the dosing feasibility of this treatment approach. Consequently, we strongly advocate further research focusing on the local pharmacokinetics of PF, particularly in the context of localized inhalation therapy.

4. Conclusions

PF, a common lung disease, results from the deterioration and scarring of lung tissue caused by a variety of factors. This pathology disrupts both the structural integrity and functional capacity of lung tissue through complex processes of tissue remodeling. The primary focus of our research was the spray drying of phytic acid, a natural chelating agent known for its minimal side effects. Formulating a dry

powder containing the zinc chelator phytic acid as Zn^{2+} is known for its key role for the activation of the bacterial enzyme LasB and mammalian MMPs. These enzymes play a critical role in the onset and progression of pulmonary fibrosis.

The final formulation contained 30 % phytic acid for chelating Zn^{2+} and thereby inhibit the actions of LasB and thus reducing a key virulence factor involved in the progressing of PF. To assess the shelf life of the particles, freshly prepared samples after spray drying were compared with samples stored in a desiccator at room temperature (20 °C) for up to 40 days. Our findings led to the conclusion that the incorporation of leucine and pH adjustment to physiological levels significantly improved shelf life by preventing agglomeration during storage. This improvement highlights the potential of the developed dry powder formulation for sustained therapeutic efficacy.

The drug loading capacity of the formulation is limited to 30 %. Higher drug amounts of phytic acid negatively influenced formulation stability and aerodynamic properties. For pulmonary application the aerodynamic properties of the dry powder particles were characterized by determining a MMAD of 3.52 μm indicating potential deep-lung deposition.

The ability of the formulation to chelate zinc ions from solution was underlined using a zinc chelation kit for both pure phytic acid and the formulated phytic acid. Following optimization, the formulation was tested for LasB inhibition, which confirmed that both pure and formulated phytic acid effectively chelated zinc, thereby inhibiting enzymes involved in PF. Additional testing for human MMP-1 and MMP-2 revealed no activity on these MMPs at the tested concentrations.

With respect to acute toxicity, reduced cell viability was observed for values >360 μg/mL for the formulated phytic acid, a concentration well above the threshold responsible for enzyme inhibition (109 μg/mL). This underlines the efficacy of the formulation in inhibiting enzymes associated with pulmonary fibrosis while maintaining a margin of safety with respect to cytotoxic effects.

CRediT authorship contribution statement

Justin Stella: Writing – review & editing, Writing – original draft, Methodology. **Maryam Ayman Mohamed Ezzat Abdelaal:** Visualization, Investigation. **Mohamed Ashraf Mostafa Kamal:** Visualization, Software. **Kristela Shehu:** Investigation, Writing – review & editing. **Alaa Alhayek:** Writing – review & editing, Investigation. **Jörg Haupenthal:** Writing – review & editing, Supervision. **Anna K. Hirsch:** Writing – review & editing. **Marc Schneider:** Writing – review & editing, Supervision, Resources, Project administration, Conceptualization.

Data availability

Data will be made available on request.

Acknowledgements

The authors would especially like to thank Jeannine Jung and Pascal Paul for performing inhibition assays and preliminary experiments for powder laser diffraction.

Supplementary materials

Supplementary material associated with this article can be found, in the online version, at doi:10.1016/j.ejps.2024.106891.

References

Aguree, S., Guo, L., Reddy, M.B., 2020. Phytic acid protects from oxidative stress induced by iron-overload and high-fat diets in ß2-microglobulin knockout mice. Molecules 25.
Alhajj, N., O'Reilly, N.J., Cathcart, H., 2021. Leucine as an excipient in spray dried powder for inhalation. Drug Discov. Today 26, 2384–2396.
Artmann, M., Staudinger, J., 2021. Inhalationstherapie bei Asthma und COPD aus physiotherapeutischer Sicht. MMW Fortschr. Med. 163, 56–64.
Badger, R.M., 1934. A relation between internuclear distances and bond force constants. J. Chem. Phys. 2, 128–131.
Bormann, T., Maus, R., Stolper, J., Tort Tarrés, M., Brandenberger, C., Wedekind, D., Jonigk, D., Welte, T., Gauldie, J., Kolb, M., Maus, U.A., 2022. Role of matrix metalloprotease-2 and MMP-9 in experimental lung fibrosis in mice. Respir. Res. 23, 180.
Bushill, J.H., Wright, W.B., Fuller, C.H.F., Bell, A.V., 1965. The crystallisation of lactose with particular reference to its occurrence in milk powder. J. Sci. Food Agric. 16, 622–628.
Buttini, F., Brambilla, G., Copelli, D., Sisti, V., Balducci, A.G., Bettini, R., Pasquali, I., 2016. Effect of flow rate on aerodynamic performance of NEXThaler® in comparison with Diskus® and Turbohaler® dry powder inhalers. J. Aerosol Med. Pulm. Drug Deliv. 29, 167–178.
Buttini, F., Colombo, G., Kwok, P.C.L., Wui, W.T., 2013. Aerodynamic Assessment for Inhalation Products: Fundamentals and Current Pharmacopoeial Methods. Inhalation Drug Delivery, pp. 91–119.
Cabral-Pacheco, G.A., Garza-Veloz, I., Castruita-De la Rosa, C., Ramirez-Acuña, J.M., Perez-Romero, B.A., Guerrero-Rodriguez, J.F., Martinez-Avila, N., Martinez-Fierro, M.L., 2020. The roles of matrix metalloproteinases and their inhibitors in human diseases. Int. J. Mol. Sci. 21, 9739.
Cares-Pacheco, M.G., Vaca-Medina, G., Calvet, R., Espitalier, F., Letourneau, J.J., Rouilly, A., Rodier, E., 2014. Physicochemical characterization of D-mannitol polymorphs: the challenging surface energy determination by inverse gas chromatography in the infinite dilution region. Int. J. Pharm. 475, 69–81.
Carvalho, T.C., Peters, J.I., Williams, R.O., 2011. Influence of particle size on regional lung deposition – what evidence is there? Int. J. Pharm. 406, 1–10.
CAS_Common_Chemistry, retrieved 2024-02-23. Phytic Acid, SciFinder.
Cauet, E., Bogatko, S., Weare, J.H., Fulton, J.L., Schenter, G.K., Bylaska, E.J., 2010. Structure and dynamics of the hydration shells of the Zn(2+) ion from ab initio molecular dynamics and combined ab initio and classical molecular dynamics simulations. J. Chem. Phys. 132, 194502.
Chatree, S., Thongmaen, N., Tantivejkul, K., Sitticharoon, C., Vucenik, I., 2020. Role of inositols and inositol phosphates in energy metabolism. Molecules 25.
Chrystyn, H., Lavorini, F., 2020. The dry powder inhaler features of the Easyhaler that benefit the management of patients. Expert Rev. Respir. Med. 14, 345–351.
Costello, A.J.R., Glonek, T., Myers, T.C., 1976. 31P Nuclear magnetic resonance-pH titrations of myo-inositol hexaphosphate. Carbohydr. Res. 46, 159–171.
Costes, L., Laoutid, F., Dumazert, L., Lopez-cuesta, J.M., Brohez, S., Delvosalle, C., Dubois, P., 2015. Metallic phytates as efficient bio-based phosphorous flame retardant additives for poly(lactic acid). Polym. Degrad. Stab. 119, 217–227.
CSID:158279, (accessed 16:38, Feb 19, 2024). Trehalose.
Dilworth, L., Stennett, D., Omoruyi, F., 2023. Cellular and molecular activities of ip6 in disease prevention and therapy. Biomolecules 13, 972.
Everett, M.J., Davies, D.T., 2021. Pseudomonas aeruginosa elastase (LasB) as a therapeutic target. Drug Discov. Today 26, 2108–2123.
Faraji, F., Mahzounieh, M., Ebrahimi, A., Fallah, F., Teymournejad, O., Lajevardi, B., 2016. Molecular detection of virulence genes in Pseudomonas aeruginosa isolated from children with Cystic Fibrosis and burn wounds in Iran. Microb. Pathog. 99, 1–4.
Fröhlich, E., Mercuri, A., Wu, S., Salar-Behzadi, S., 2016. Measurements of deposition, lung surface area and lung fluid for simulation of inhaled compounds. Front. Pharmacol. 7.
Gabardi, S., Carter, D., Martin, S., Roberts, K., 2011. Recommendations for the proper use of nonprescription cough suppressants and expectorants in solid-organ transplant recipients. Prog. Transplant. 21, 6–13.
Gagne, O.C., Hawthorne, F.C., 2020. Bond-length distributions for ions bonded to oxygen: results for the transition metals and quantification of the factors underlying bond-length variation in inorganic solids. IUCrJ 7, 581–629.
Ganaie, T.A., Masoodi, F.A., Rather, S.A., Gani, A., 2021. Exploiting maltodextrin and whey protein isolate macromolecules as carriers for the development of freeze dried honey powder. Carbohydr. Polym. Technol. Appl. 2, 100040.
Glass, D.S., Grossfeld, D., Renna, H.A., Agarwala, P., Spiegler, P., DeLeon, J., Reiss, A.B., 2022. Idiopathic pulmonary fibrosis: current and future treatment. Clin. Respir. J. 16, 84–96.
Gosselin, R.E., Coghlan, E.R., 1953. The stability of complexes between calcium and orthophosphate, polymeric phosphate, and phytate. Arch. Biochem. Biophys. 45, 301–311.
Gupta, R.K., Gangoliya, S.S., Singh, N.K., 2015. Reduction of phytic acid and enhancement of bioavailable micronutrients in food grains. J. Food Sci. Technol. 52, 676–684.
Harvey, P.R., Tarran, R., Garoff, S., Myerburg, M.M., 2011. Measurement of the airway surface liquid volume with simple light refraction microscopy. Am. J. Respir. Cell Mol. Biol. 45, 592–599.
Haynes, W.M., Lide, D.R., Bruno, T.J., 2016. CRC Handbook of Chemistry and Physics: a Ready-Reference Book of Chemical and Physical Data, 2016-2017 97th Edition ed. CRC Press, Boca Raton, Florida.
Himstedt, A., Braun, C., Wicha, S.G., Borghardt, J.M., 2020. Towards a quantitative mechanistic understanding of localized pulmonary tissue retention—a combined *in vivo*/in silico approach based on four model drugs. Pharmaceutics 12, 408.
Huang, E., Peng, N., Xiao, F., Hu, D., Wang, X., Lu, L., 2020. The roles of immune cells in the pathogenesis of fibrosis. Int. J. Mol. Sci. 21, 5203.
Inoue, R., Yasuma, T., Fridman D'Alessandro, V., Toda, M., Ito, T., Tomaru, A., D'Alessandro-Gabazza, C.N., Tsuruga, T., Okano, T., Takeshita, A., Nishihama, K., Fujimoto, H., Kobayashi, T., Gabazza, E.C., 2023. Amelioration of pulmonary fibrosis by matrix metalloproteinase-2 overexpression. Int. J. Mol. Sci. 24, 6695.

Kamp, D.W., Israbian, V.A., Yeldandi, A.V., Panos, R.J., Graceffa, P., Weitzman, S.A., 1995. Phytic acid, an iron chelator, attenuates pulmonary inflammation and fibrosis in rats after intratracheal instillation of asbestos. Toxicol. Pathol. 23, 689–695.
Kany, A.M., Sikandar, A., Yahiaoui, S., Haupenthal, J., Walter, I., Empting, M., Köhnke, J., Hartmann, R.W., 2018. Tackling pseudomonas aeruginosa virulence by a hydroxamic acid-based LasB inhibitor. ACS Chem. Biol. 13, 2449–2455.
Kapral, M., Wawszczyk, J., Jurzak, M., Hollek, A., Węglarz, L., 2012. The effect of inositol hexaphosphate on the expression of selected metalloproteinases and their tissue inhibitors in IL-1β-stimulated colon cancer cells. Int. J. Colorectal Dis. 27, 1419–1428.
Kolling, D., Haupenthal, J., Hirsch, A.K.H., Koehnke, J., 2023. Facile production of the pseudomonas aeruginosa virulence factor LasB in escherichia coli for structure-based drug design. Chembiochem 24, e202300185.
Konstantinovic, J., Kany, A.M., Alhayek, A., Abdelsamie, A.S., Sikandar, A., Voos, K., Yao, Y., Andreas, A., Shafiei, R., Loretz, B., Schonauer, E., Bals, R., Brandstetter, H., Hartmann, R.W., Ducho, C., Lehr, C.M., Beisswenger, C., Muller, R., Rox, K., Haupenthal, J., Hirsch, A.K.H., 2023. Inhibitors of the Elastase LasB for the treatment of pseudomonas aeruginosa lung infections. ACS Cent. Sci. 9, 2205–2215.
Korn, C., Balbach, S., 2014. Compound selection for development – Is salt formation the ultimate answer? Experiences with an extended concept of the "100mg approach". Eur. J. Pharm. Sci. 57, 257–263.
Laronha, H., Caldeira, J., 2020. Structure and function of human matrix metalloproteinases. Cells 9, 1076.
Li, L., Sun, S., Parumasivam, T., Denman, J.A., Gengenbach, T., Tang, P., Mao, S., Chan, H.K., 2016. L-Leucine as an excipient against moisture on *in vitro* aerosolization performances of highly hygroscopic spray-dried powders. Eur. J. Pharm. Biopharm. 102, 132–141.
Littringer, E.M., Mescher, A., Eckhard, S., Schröttner, H., Langes, C., Fries, M., Griesser, U., Walzel, P., Urbanetz, N.A., 2012. Spray drying of mannitol as a drug carrier—the impact of process parameters on product properties. Dry. Technol. 30, 114–124.
Lv, Y., Zhang, Z., Hou, L., Zhang, L., Zhang, J., Wang, Y., Liu, C., Xu, P., Liu, L., Gai, X., Lu, T., 2015. Phytic acid attenuates inflammatory responses and the levels of NF-κB and p-ERK in MPTP-induced Parkinson's disease model of mice. Neurosci. Lett. 597, 132–136.
Mah, P.T., O'Connell, P., Focaroli, S., Lundy, R., O'Mahony, T.F., Hastedt, J.E., Gitlin, I., Oscarson, S., Fahy, J.V., Healy, A.M., 2019. The use of hydrophobic amino acids in protecting spray dried trehalose formulations against moisture-induced changes. Eur. J. Pharm. Biopharm. 144, 139–153.
Moghoofei, M., Mostafaei, S., Kondori, N., Armstrong, M.E., Babaei, F., 2022. Bacterial and viral coinfection in idiopathic pulmonary fibrosis patients: the prevalence and possible role in disease progression. BMC Pulm. Med. 22, 60.
Ng, L.H., Ling, J.K.U., Hadinoto, K., 2022. Formulation strategies to improve the stability and handling of oral solid dosage forms of highly hygroscopic pharmaceuticals and nutraceuticals. Pharmaceutics 14, 2015.
Nielsen, G.D., Koponen, I.K., 2018. Insulation fiber deposition in the airways of men and rats. A review of experimental and computational studies. Regul. Toxicol. Pharmacol. 94, 252–270.
Oatway, L., Vasanthan, T., Helm, J.H., 2001. Phytic acid. Food Rev. Int. 17, 419–431.
Ohrem, H.L., Schornick, E., Kalivoda, A., Ognibene, R., 2014. Why is mannitol becoming more and more popular as a pharmaceutical excipient in solid dosage forms? Pharm. Dev. Technol. 19, 257–262.
Ortiz, S.R., Heinz, A., iller, K., Field, M.S., 2022. Erythritol Synthesis in Human Cells is Elevated in Response to Oxidative Stress and Regulated By the Non-Oxidative Pentose Phosphate Pathway. bioRxiv, 2022.2003.2007.483290.
Pardo, A., Cabrera, S., Maldonado, M., Selman, M., 2016. Role of matrix metalloproteinases in the pathogenesis of idiopathic pulmonary fibrosis. Respir. Res. 17, 23.
Procaccini, C., De Rosa, V., Perna, F., Matarese, G., 2019. Chapter 2 - complex interface between immunity and metabolism: the lung as a target organ. Johnston, R.A., Suratt, B.T. (Eds.). Mechanisms and Manifestations of Obesity in Lung Disease. Academic Press, pp. 23–43.
Ratjen, F., Rietschel, E., Kasel, D., Schwiertz, R., Starke, K., Beier, H., van Koningsbruggen, S., Grasemann, H., 2006. Pharmacokinetics of inhaled colistin in patients with cystic fibrosis. J. Antimicrob. Chemother. 57, 306–311.
Ruge, C.A., Kirch, J., Canadas, O., Schneider, M., Perez-Gil, J., Schaefer, U.F., Casals, C., Lehr, C.M., 2011. Uptake of nanoparticles by alveolar macrophages is triggered by surfactant protein A. Nanomed. Nanotechnol. Biol. Med. 7, 690–693.
Rundfeldt, C., Steckel, H., Scherliess, H., Wyska, E., Wlaź, P., 2013. Inhalable highly concentrated itraconazole nanosuspension for the treatment of bronchopulmonary aspergillosis. Eur. J. Pharm. Biopharm. 83, 44–53.
Saint-Criq, V., Villeret, B., Bastaert, F., Kheir, S., Hatton, A., Cazes, A., Xing, Z., Sermet-Gaudelus, I., Garcia-Verdugo, I., Edelman, A., Sallenave, J.M., 2018. Pseudomonas aeruginosa LasB protease impairs innate immunity in mice and humans by targeting a lung epithelial cystic fibrosis transmembrane regulator–IL-6–antimicrobial–repair pathway. Thorax 73, 49.
Sartorius_AG, 2018. Operating Instructions-Sartorius Moisture Analyzer.
Silva, E.O., Bracarense, A.P.F.R.L., 2016. Phytic acid: from antinutritional to multiple protection factor of organic systems. J. Food Sci. 81, R1357–R1362.
Sosnik, A., Seremeta, K.P., 2015. Advantages and challenges of the spray-drying technology for the production of pure drug particles and drug-loaded polymeric carriers. Adv. Colloid Interface Sci. 223, 40–54.
Sou, T., Forbes, R.T., Gray, J., Prankerd, R.J., Kaminskas, L.M., McIntosh, M.P., Morton, D.A.V., 2016. Designing a multi-component spray-dried formulation platform for pulmonary delivery of biopharmaceuticals: the use of polyol, disaccharide, polysaccharide and synthetic polymer to modify solid-state properties for glassy stabilisation. Powder Technol. 287, 248–255.
Speca, S., Dubuquoy, C., Rousseaux, C., Chavatte, P., Desreumaux, P., Spagnolo, P., 2020. GED-0507 is a novel potential antifibrotic treatment option for pulmonary fibrosis. Cell. Mol. Immunol. 17, 1272–1274.
Voshaar, T., 2005. Moderne inhalationstherapien. suspension, lösung oder pulver? Entscheidend ist die richtige Technik [Modern inhalation therapy]. MMW Fortschr. Med. 147, 46–48.
Yamazaki, R., Nishiyama, O., Sano, H., Iwanaga, T., Higashimoto, Y., Kume, H., Tohda, Y., 2016. Clinical features and outcomes of IPF patients hospitalized for pulmonary infection: a Japanese cohort study. PLoS One 11, e0168164.